Tyrosinase-catalyzed oxidation of fluorophenols

Battaini, G.; Monzani, E.; Casella, L.; Lonardi, E.; Tepper, A.W.J.W.; Canters, G.W.; Bubacco, L.

Note: To cite this publication please use the final published version (if applicable).

Tyrosinase-catalyzed Oxidation of Fluorophenols*

Giuseppe Battaini‡, Enrico Monzani‡, Luigi Casella‡§, Emanuela Lonardi¶, Armand W. J. W. Tepper¶, Gerard W. Canters¶, and Luigi Bubacco‖

From the ‡Dipartimento di Chimica Generale, Università di Pavia, Via Taramelli 12, 27100 Pavia, Italy, the ¶Leiden Institute of Chemistry, Gorlaeus Laboratories, Leiden University, Einsteinweg 55, 2333 CC, Leiden, The Netherlands, and the ‖Dipartimento di Biologia, Università di Padova, Via Trieste 75, 3012 Padova, Italy

The activity of the type 3 copper enzyme tyrosinase toward 2-, 3-, and 4-fluorophenol was studied by kinetic methods and ^{1}H and ^{19}F NMR spectroscopy. Whereas 3- and 4-fluorophenol react with tyrosinase to give products that undergo a rapid polymerization process, 2-fluorophenol is not reactive and actually acts as a competitive inhibitor in the enzymatic oxidation of 3,4-dihydroxyphenylalanine (L-dopa). The tyrosinase-mediated polymerization of 3- and 4-fluorophenols has been studied in detail. It proceeds through a phenolic coupling pathway in which the common reactive fluoroquinone, produced stereospecifically by tyrosinase, eliminates an inorganic fluorine ion. The enzymatic reaction studied as a function of substrate concentration shows a prominent lag that is completely depleted in the presence of L-dopa. The kinetic parameters of the reactions can be correlated to the electronic and steric effects of the fluorine substituent position. Whereas the fluorine electron withdrawing effect appears to control the binding of the substrates (K_m for 3- and 4-fluorophenols and K_I for 2-fluorophenol), the k_{cat} parameters do not follow the expected trend, indicating that in the transition state some additional steric effect rules the reactivity.

Tyrosinases (Tys)[1] are monooxygenating enzymes that catalyze the *ortho*-hydroxylation of monophenols and the subsequent oxidation of diphenols to quinones (1). The reaction is widespread in nature, from bacteria to fungi, plants, and mammals. In mammals, when L-tyrosine acts as the substrate, the formed quinones are reactive precursors in the synthesis of melanin pigments. In fruits, vegetables, and mushrooms, Ty is a fundamental enzyme in the browning process that occurs during product storage and upon bruising. Ty contains a dinuclear type 3 copper center, in which two copper ions are closely spaced and coordinated each by three histidines through the N-ε nitrogen atoms (1). This type of site has been found and structurally characterized also in hemocyanins, which act as oxygen carriers in arthropods and mollusks (2–4),

and in catechol oxidases, which perform the oxidation of *o*-diphenols to quinones (5). The reasons why these proteins perform different functions, although their catalytic sites appear to be similar both in structure and oxygen binding ability, remains to be clarified (6). During activity, the type 3 site of Ty can exist in three main redox forms: (*a*) Ty$_{deoxy}$ [Cu(I) Cu(I)], the reduced species which binds oxygen to give (*b*) Ty$_{oxy}$ [Cu(II)-O$_2^{2-}$-Cu(II)], in which molecular oxygen is bound as peroxide in a μ-η²:η² side-on bridging mode, and (*c*) Ty$_{met}$ [Cu(II)-Cu(II)], the resting form of the enzyme, where the Cu^{2+} ions are normally bridged by a small ligand (7, 8). The cloning technique, developed recently, and more detailed kinetic studies (6–12) have increased the current understanding of Ty mechanism and structure. Additional studies (8, 13–16) on inhibitors also provided structural information. The importance of the latter studies is related to the considerable interest of Tys from the medical, agricultural, and industrial point of view. For instance, Ty inhibitors are of great concern in the cosmetic industry (17) and in food technology as anti-browning agents (18, 19). Moreover, the tyrosinases present in soil have been found recently to be involved in the formation of humus through random coupling of different aromatic compounds. These findings have attracted interest in the activity of Ty as a potential detoxifying agent for xenobiotic compounds with phenolic structure (20, 21). In this paper we report a mechanistic and kinetic study on the activity of Ty from *Streptomyces antibioticus* toward the three isomeric fluorophenols, an important class of xenobiotic substances. The number of fluorine-containing environmental contaminants has strongly increased during the past decade (22), and the polymerization processes mediated by Tys can therefore contribute to soil clean up and water treatment.

EXPERIMENTAL PROCEDURES

Chemicals—The enzyme was prepared from the growth medium liquid cultures of *S. antibioticus,* harboring the pIJ703 expression plasmid, and purified according to published procedures (13). Protein concentrations were determined optically using a value of 82 mM^{-1} cm^{-1} for the extinction coefficient at 280 nm (23). Commercial 2-fluorophenol, 3-fluorophenol, and 4-fluorophenol, obtained from Sigma, were freshly purified by HPLC as reported below. All other reagents were purchased from commercial sources and used as received unless otherwise noted. Electrospray ionization MS spectra were acquired using a Finnigan MAT system equipped with an ion trap detector. The solution was introduced into the electrospray source at 10 μl min^{-1} using a syringe pump instrument. The ESI source was operated at 3.5 kV; the capillary temperature was set at 180 °C and its voltage at 10 V; and the experiments were recorded both in positive and negative ion mode. HPLC analysis and purifications were performed loading 1 ml of samples onto Supelco LC18 semipreparative column (250 × 10 mm). Elution was carried out at 5 ml/min starting with pure water and continuing elution with water for 4 min, followed by a linear gradient from 0 to 100% acetonitrile in 20 min. Spectrophotometric detection of HPLC elution profile in the range 200–650 nm was performed with a Jasco MD-1510 diode array. ^{19}F NMR measurements were obtained on a Bruker

§ To whom correspondence should be addressed: Dipartimento di Chimica Generale, Università di Pavia, Via Taramelli 12, 27100 Pavia, Italy. Tel.: 39-0382-507331; Fax: 39-0382-528544; E-mail: bioinorg@unipv.it.

[1] The abbreviations used are: Ty, tyrosinase; L-dopa, 3,4-dihydroxyphenylalanine; FP, fluorophenol; *m*-FP, 3-fluorophenol; *p*-FP, 4-fluorophenol; *o*-FP, 2-fluorophenol; HPLC, high pressure liquid chromatography; ESI-MS, electrospray ionization-mass spectrometry.
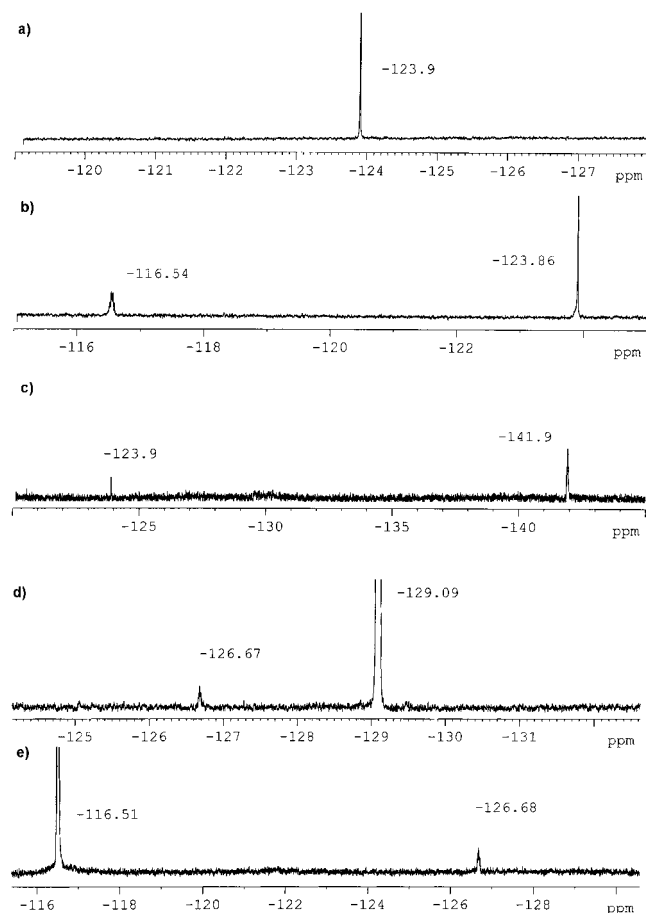
FIG. 1. **^{19}F NMR spectra of the incubation mixtures, after 6-h reaction time at 25 °C, of Ty (0.4 μM) and *p*-FP (1 mM) (*a*); *m*-FP (1 mM) (*b*); *o*-FP (1 mM) (*c*); *p*-FP (1 mM) and ascorbic acid (1 mM) (*d*); and *m*-FP (1 mM) and ascorbic acid (1 mM) (*e*).** All the reactions were carried out in 100 mM phosphate buffer, pH 6.8.
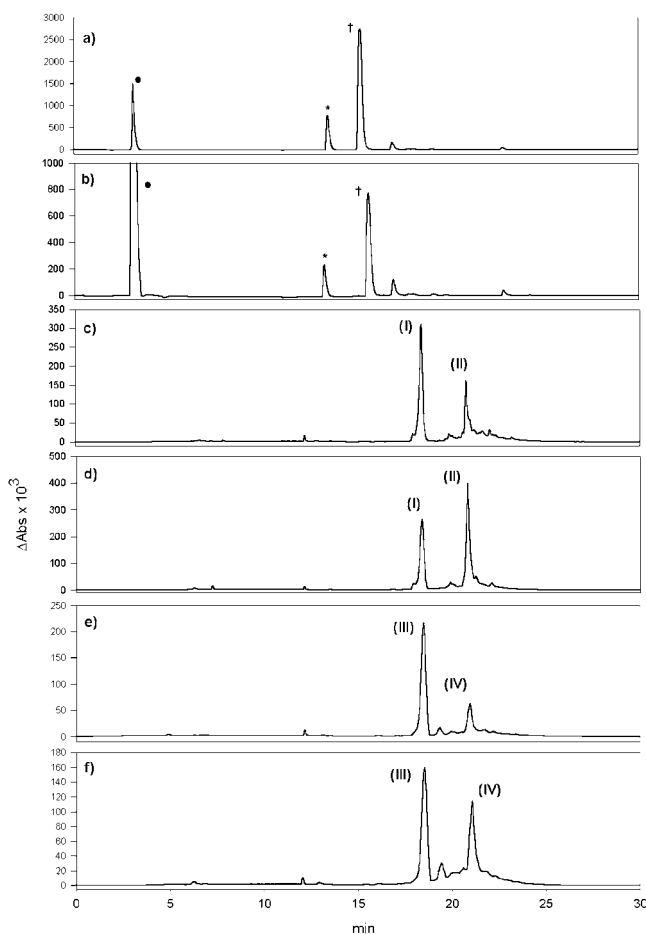

FIG. 2. *a*, HPLCs of incubation mixtures of Ty (0.1 μM) with *p*-FP (1 mM) and ascorbic acid (1 mM); *b*, *m*-FP (1 mM) and ascorbic acid (1 mM), after a 2-h reaction time, monitored at 280 nm. The *peak* marked with an *asterisk* was identified as the fluorocatechol derivative that forms under these conditions; the other peaks in *a* and *b* correspond to the starting phenol (†) and ascorbic acid (●). The other chromatograms contain traces monitored at 420 nm corresponding to samples of *p*-FP (1 mM) after 30 min reaction time (*c*), *p*-FP (1 mM) after 60 min (*d*), *m*-FP (1 mM) after 30 min (*e*), and *m*-FP (1 mM) after 60 min (*f*). All incubations were in 100 mM phosphate buffer, pH 6.8, at 25 °C.

AVANCE spectrometer operating at proton Larmor frequency of 400.13 MHz. The temperature was set at 25 °C. The spectral width was between 20,000 and 50,000 Hz depending on the sample of interest. The number of data points was 64,000 for a typical 128 scans experiment. Fluorine chemical shifts are reported relative to CFCl$_3$.

Incubation Conditions—The reactions were performed with 0.4 μM Ty (final concentration after 4 additions) and 1 mM fluorophenol in 100 mM phosphate buffer, pH 6.8, at 25 °C. The mixtures were magnetically stirred in open vessels in order to maintain the solution saturated with atmospheric oxygen. In the semipreparative experiments carried out for 6 h, the enzyme was always activated by 0.4 μM L-dopa, which was added in four portions in combination with Ty. In the experiments carried out under reducing conditions, 1 mM ascorbic acid was added. After 6 h of reaction time, the mixtures were centrifuged for 5 min, and either trifluoroacetic acid (0.5 mM), for ^{19}F NMR measurements, or *p*-hydroxyphenylpropionic acid (1 mM), for HPLC analysis, was added as internal standard to the solutions. Samples used for NMR contained 5% D$_2$O for locking the magnetic field. The data are discussed in terms of the percentage of substrate transformed (%Tr) and percentage of fluorine released from the aromatic ring (%F). %Tr was determined by HPLC analysis, in which the unreacted phenols were quantified by comparison to the internal standard. %F was estimated by ^{19}F NMR analysis, by integration of the detected peaks with respect to the internal standard.

For detection of the polymerization intermediates, the same reaction conditions were maintained, but Ty concentration was reduced to 0.1 μM. Samples of the reaction mixtures (1 ml) were withdrawn after 30 min, 1 h, and 2 h and were directly injected into the HPLC column. The standard incubation volume of 1 ml was increased to 10 ml to enable the isolation of sufficient material for spectral characterization of the coupling products. The reactions were stopped after 30 min, for the first intermediates (**I** or **III**), or after 1 h, for the second intermediate (**II** or **IV**), in the reactions of *p*-FP and *m*-FP, respectively, by cooling the

sample in ice and extracting the solutions 4 times with 2 ml of ethyl acetate. The combined organic extracts were rotary-evaporated to dryness, and the resulting purple solid material was dissolved in 1 ml of acetonitrile/water, 80:20 (v/v). The solution was further purified by HPLC, and the fractions containing the intermediate of interest were collected, dried, and analyzed.

Kinetic Experiments—Kinetic studies on the catalytic oxidation of fluorophenols were performed in 100 mM phosphate buffer, pH 6.8, saturated with air, using a magnetically stirred and thermostated cell with 1-cm optical path length, at 25 ± 0.1 °C. In the experiments where the oxidation rate was studied as a function of FP concentrations, Ty was kept at 0.04 μM, whereas the concentration of the substrates was varied between 1 and 90 mM for *p*-FP and 0.5 and 60 mM for *m*-FP. Different sets of experiments were performed in order to establish the dependence of the initial lag of the reaction by L-dopa concentration. Thus, the concentration of L-dopa was varied between 0 and 1 μM, for which the lag phase was completely depleted. Formation of the quinone moieties (**I** and **III**) was monitored through the development of their characteristic optical band at 420 nm ($\epsilon \cong 2000$ M^{-1} cm^{-1}). The noise during the measurements was reduced by reading the difference in absorbance between 420 and 800 nm (at the latter wavelength absorbance change during the reaction was only due to noise). The initial rates (v_0) were obtained by fitting linearly, normally between 100- and 300-s reaction time, the ΔA *versus* time plots. In the inhibition studies, the concentration of *o*-PF was kept fixed (at 0, 10, 20, 35, and 60 mM) and that of L-dopa was varied between 1 and 10 mM, whereas Ty concentration was always kept at 0.04 μM. Dopachrome formation was moni-

TABLE I

Characterization data for the intermediates isolated in the enzymatic oxidation of p-FP and m-FP

	HPLC elution time	ESI-mass	^{1}H NMR	^{19}F NMR (ppm)
	min	*m/z*	*ppm*	*(ppm)*
I	18.5	$[219.1]^+$	7.03 (*m*), 6.88 (*m*), 6.73 (*d*), 6.46 (*d*), 6.31 (*dd*)	−124.72(*m*)
II	21	$[329.7]^+$, $[351.7]^+$	7.45 (*m*), 7.15 (*m*), 6.5 (*s*)	−125.35(*m*)
III	18.6	$[219.1]^+$	7.31 (*m*), 6.71 (*m*), 6.42 (*d*), 6.28 (*dd*)	−112.31(*m*)
IV	21.3	$[329.7]^+$, $[351.7]^+$	NM	NM

The abbreviations used are: *m,* multiplet; *d,* doublet; *dd,* doublet of doublets; *s,* singlet; NM, not measured.
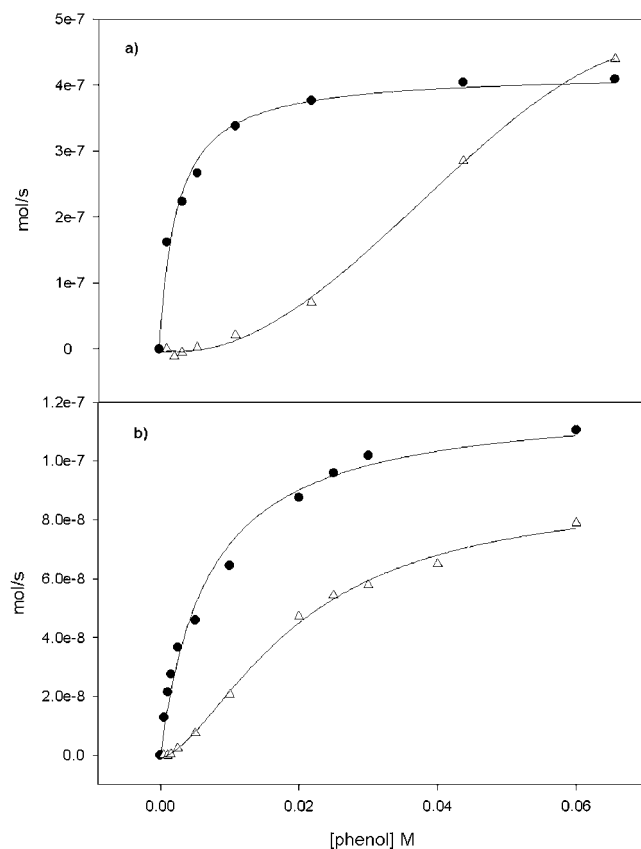

FIG. 3. **Kinetic plots of the initial oxidation rates of the fluorophenols as a function of substrate concentration in the presence of 1 μM L-dopa (●) and without L-dopa (△).** Ty concentration was kept at 0.04 μM, whereas substrate concentrations varied between 1 and 90 mM for *p*-FP (*a*) and 0.5 and 60 mM for *m*-FP (*b*).
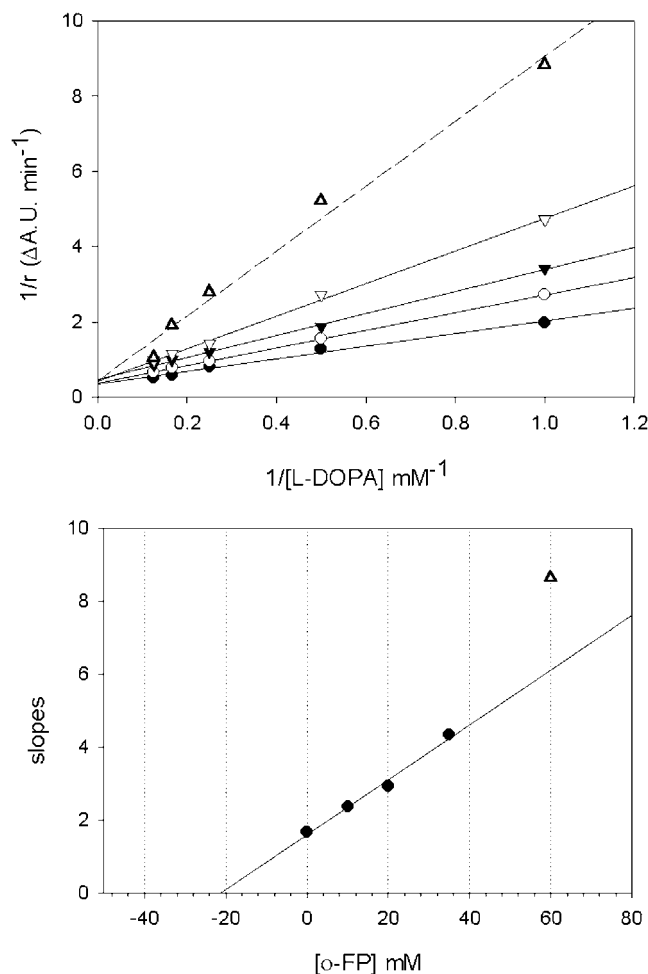

FIG. 4. **Double-reciprocal plots of the kinetics of *o*-FP inhibition for the Ty-catalyzed oxidation of L-dopa measured in 100 mM phosphate buffer at pH 6.8 and 25 °C and the corresponding replots of the slopes *versus o*-FP concentrations.**

tored through the development of its characteristic optical band at 475 nm (ϵ = 3600 M^{-1} cm^{-1}).

NMR Spectroscopy—Ty$_{met}$ samples for NMR studies ($\sim$0.6 mM in 100 mM phosphate buffer at pH 6.80) were prepared as described before (7). *o*-FP was added to the protein samples from concentrated stock solutions prepared by using the same buffer. Protein ^{1}H NMR spectra were recorded at 600 MHz using a Bruker DMX-600 spectrometer and the super-WEFT pulse sequence (24). Depending on the required signal to noise ratio, 4,000 to 32,000 FIDs were recorded, Fourier-transformed using a 60-Hz exponential window function (LB), and base line-corrected using the Bruker provided software.

RESULTS

S. antibioticus Ty produces different effects when reacted with the three isomeric mono-fluorophenols in solution. Whereas a rapid browning can be observed for 3-fluorophenol (*m*-FP) and 4-fluorophenol (*p*-FP), 2-fluorophenol (*o*-FP) did not undergo any apparent reaction. The reaction of *m*-FP and *p*-FP in the presence of Ty for a few hours produced a large amount of dark brown solid product, which appeared to be insoluble in common organic solvents like Me$_2$SO, CH$_2$Cl$_2$, and ethyl ace-

tate. The HPLC and ^{19}F NMR analyses performed on the supernatant solution, after centrifugation of the insoluble polymer, displayed different product patterns for different substrates. In the case of *p*-FP, the ^{19}F NMR spectrum shown in Fig. 1*a* exhibits only the presence of inorganic fluorine (−123.9 ppm), which can be estimated to be about 50% of the starting phenol. The nearly complete consumption of *p*-FP was confirmed by HPLC analysis, where only 2% of the starting fluorophenol was detected after 6 h of Ty reaction. In the same reaction conditions, almost 30% *m*-FP remained unreacted. This is shown in the ^{19}F NMR spectrum in Fig. 1*b*, where two peaks, at −116.54 ppm and −123.86 ppm, are present. The former peak, with a multiplet structure shape, corresponds to 30% unreacted *m*-FP, whereas the second peak corresponds to inorganic fluorine and accounts for 35% of the initial phenol concentration. Solutions of *o*-FP are very little
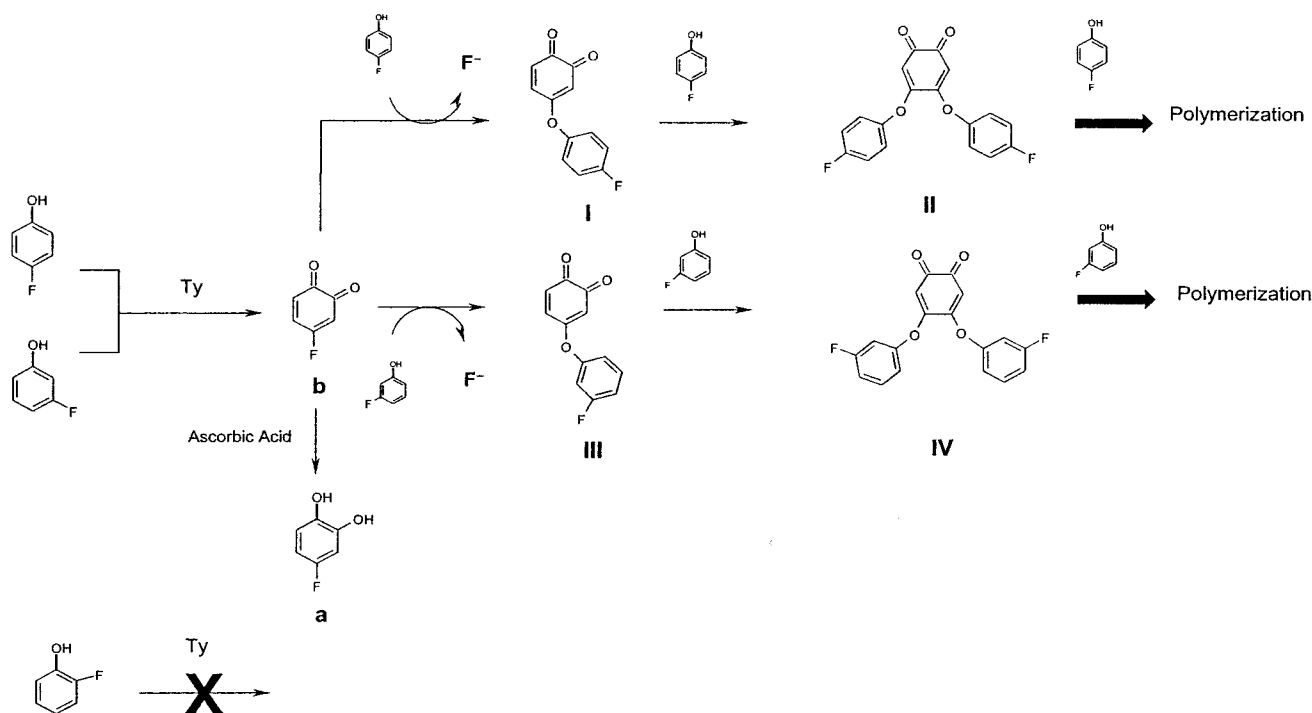
SCHEME 1

affected by incubations with Ty. Only about 5% of starting phenol was consumed after a long reaction with the enzyme, and only traces of inorganic fluorine were detected in the ^{19}F NMR spectrum (Fig. 1*c*).

When the enzymatic reactions of *m*-FP and *p*-FP were carried out in the presence of ascorbic acid, the browning effect was completely quenched. The HPLCs of the reaction mixtures reveal the formation of new species common to both the substrates (Fig. 2, *a* and *b*). No other products were identified even on extending the reaction times up to 8 h. The ^{19}F NMR spectra of the reaction mixtures show, besides the peak of the starting phenol, the presence of a resonance at -126.67 ppm (Fig. 1, *d* and *e*), unequivocally assigned to the same *o*-catechol derivative in both cases according to the data reported in the literature (25). The negative ion ESI-MS analysis of both reaction mixtures from *m*-FP and *p*-FP exhibit two clusters of peaks at 127.3 *m/z* and 149.0 *m/z*, which can be attributed to the $[\text{F-catechol} - \text{H}^+]^-$ and $[\text{F-catechol} - 2\text{H}^+ + \text{Na}^+]^-$ species, respectively. The lack of reactivity of *o*-FP mentioned above was confirmed by the experiment carried out in the presence of ascorbic acid.

In order to characterize the products formed in the early steps of the polymerization reaction undergone by *m*-FP and *p*-FP, the browning process was followed by HPLC analysis at different reaction times. Taking into account that significant scattering of the solution, which indicates the occurrence of polymer precipitation, normally starts after 2 h of enzymatic reaction, three samples of the reaction mixture were analyzed for both *m*-FP and *p*-FP reactions after 30-, 60-, and 120-min reaction times. The optical detection of the products in the wavelength range between 200 and 600 nm revealed the formation and time evolution of three major species, which share a broad absorption band at 420 nm. These products were successfully separated, and their HPLC traces detected at 420 nm, reported in Fig. 2, *c* and *d*, refer to the products obtained from *p*-FP, whereas *e* and *f* refer to those resulting from *m*-FP. Initially, the enzymatic reaction rapidly gives rise to the product with a retention time of 18.5 min (**I**) for the *p*-FP reaction and 18.6 min (**III**) for the *m*-FP reaction. These products
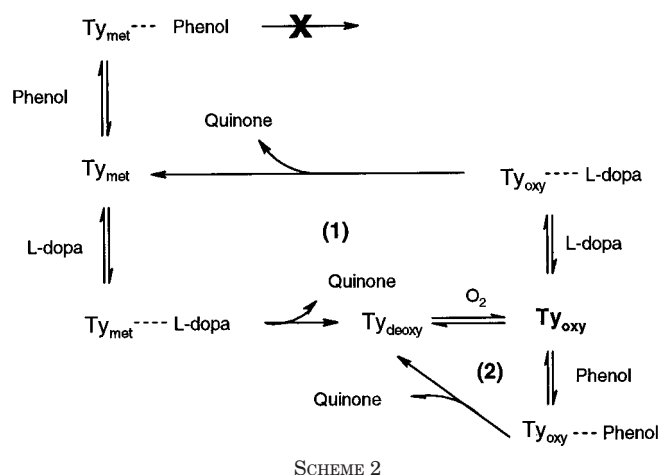
evolved in times of the order of 1 h into two different species, which were still characterized by an optical absorption band at 420 nm but had different retention times as follows: 21.0 min (**II**) for the *p*-FP reaction and 21.3 min (**IV**) for the *m*-FP reaction, respectively. After 2 h of reaction time, polymer precipitation involved the products associated with peaks **II** and **IV**; these peaks decreased in intensity until they completely disappeared. The browning processes, related to the formation of compounds I–IV, were not observed without the enzyme.

In order to define the structure of the four intermediates detected by HPLC as described above, semipreparative scale reactions were performed. Samples of the reaction mixtures were quenched at different times, corresponding to maximum formation of intermediates **I** and **II** (for the *p*-FP reaction) and **III** and **IV** (for the *m*-FP reaction) and extracted with ethyl acetate. The extracts were further purified by HPLC and the products analyzed by ESI-MS, ^{1}H NMR, and ^{19}F NMR spectroscopy; the data are shown in the Table I. The low concentration in which **IV** is produced prevented its NMR characterization.

The dimeric compounds **I** and **III** maintain the quinone structure and exhibit a moderately intense absorption band at 420 nm ($\epsilon \approx 2000$ M^{-1} cm^{-1}). The mass peaks at *m/z* 219.1 observed for these species represent the $[\textbf{I/III} + \text{H}]^+$ ions, and their ^{1}H NMR spectra contain an ABX pattern that is consistent with the structure shown in Scheme 1.

The trimeric intermediates **II** and **IV** exhibit optical properties similar to those of **I** and **III** but with a maximum shifted to 415 nm. The structure shown in Scheme 1 is consistent with their spectral data (Table I), where the MS peaks at *m/z* 329.7 and 351.7 refer to the ions $[\textbf{II/IV} + \text{H}]^+$ and $[\textbf{II/IV} + \text{Na}]^+$, respectively. The ^{1}H NMR spectrum of **II**, besides the aromatic envelope, shows a characteristic singlet, which could be attributed to the equivalent protons of the symmetric quinone moiety.

Kinetic measurements of the Ty activity toward the reactive fluorophenols *m*-FP and *p*-FP were carried out at 420 nm as a function of substrate concentration. The absorbance *versus* time curves showed an induction period that can last more than

SCHEME 2

FIG. 5. **Hammett plot of K_m, for m-FP and p-FP, and K_I, for o-FP, where the σ scale has been calculated as the log (K_{aF}/K_{aH}); with K_{aF} and K_{aH} representing the acidity constant of fluorophenols and a nonsubstituted phenol, respectively (31).**

600 s and decreases with the increase of substrate concentration. The resulting plots of initial rates *versus* substrate concentration exhibited a sigmoidal shape because of the prominent induction period at low concentration of fluorophenols (Fig. 3).

When the kinetic analysis was performed in the presence of at least 25-fold excess L-dopa, with respect to the enzyme concentration, the observed behavior changed completely. The lag phase previously observed in the enzymatic reactions without L-dopa markedly reduced to less than 100 s. The resulting plots of initial rates after the induction period *versus* substrate concentrations showed for both p-FP and m-FP a simple substrate saturation dependence. The kinetic parameters obtained in these conditions for the enzymatic reactions are shown in Reactions 1 and 2,

$$p\text{-FP}, \; k_{cat} \; = \; 10.5 \pm 0.3 \; s^{-1} \quad K_m \; = \; 2.9 \pm 0.4 \; \text{mM}$$

REACTION 1

$$m\text{-FP}, \; k_{cat} \; = \; 3.0 \pm 0.2 \; s^{-1} \quad K_m \; = \; 6.9 \pm 0.9 \; \text{mM}$$

REACTION 2

As discussed above, o-FP does not react appreciably with Ty and actually it acts as an inhibitor of L-dopa enzymatic oxidation. The inhibition behavior of o-FP, studied by changing both the L-dopa and o-FP concentrations, is reported in Fig. 4. This analysis allowed us to establish that the inhibition mechanism is competitive and to estimate the inhibition constant (K_I) as 20.0 mM. It is also noteworthy that increasing the o-FP concentration above 40 mM produces reproducible deviation from linearity of the slope *versus* [o-FP] plot. Although we did not study this effect in detail, it is possible that more than one molecule of o-FP interacts with the enzyme in these conditions.

Fig. 6 shows the effect of saturating concentration of o-FP on the ^{1}H NMR spectrum of the resting Ty$_{met}$ form. Although the Cu(II)-Cu(II) ground state of the enzyme is diamagnetic (S = 0), the paramagnetic (S = 1) triplet state is appreciably populated at room temperature and provides enough paramagnetic shift to the nuclei in the dicopper environment (26). As reported previously (7, 8, 13), these signals originate from the nuclei of the coordinated His residues. Therefore, the region between 15 and 50 ppm represents a detailed fingerprint of the type 3 copper site environment which appears to be very sensitive to changes in both copper geometry and ligand binding (7, 8, 13). Binding of the exogenous o-FP ligand to the dicopper(II) enzyme is suggested by the shifts observed for some of the paramagnetic signals.
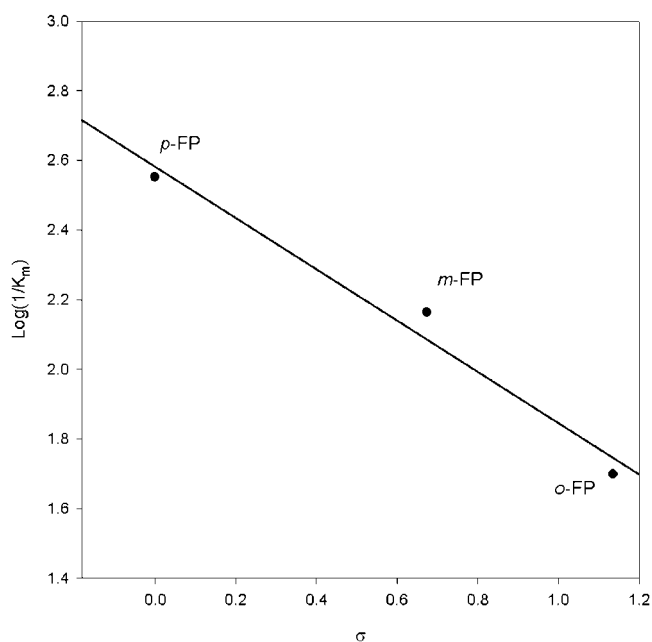
DISCUSSION

S. antibioticus tyrosinase reacts differently with the three isomeric mono-fluorophenols, whereas m-FP and p-FP undergo extensive browning and precipitation reactions, o-FP does not react appreciably with the enzyme. The reaction occurring with the former substrates starts with an initial hydroxylation and a successive oxidation to form the intermediates indicated as **a** and **b** in Scheme 1.

The quinone initially formed is extremely reactive and undergoes fast (nonenzymatic) coupling reactions with the phenols present in the solution. Through this reaction one molecule of inorganic fluorine is produced. The dimeric compounds **I**, from p-FP, and **III**, from m-FP, represent the major product species in solution at intermediate reaction times (about 30 min). The early enzymatic steps preceding formation of **I** and **III** can be followed only in the presence of a reducing agent like ascorbic acid. The isolation and the spectroscopic characterization of a common catechol intermediate, **a**, in the reactions of p-FP and m-FP indicates that Ty performs a stereospecific hydroxylation of m-FP in *para* position to the fluorine substituent. The fluorine dipolar field effect plays a major role in selecting the position of electrophilic attack, making the other available site electronically poor. Moreover, detection of compound **a** indirectly but unequivocally proves that quinone **b** acts as the initiator of the polymerization process. The dimeric compounds **I** and **III** are still reactive on their turn. They accumulate in sizable amount during the initial reaction time, after which they are partially consumed by the second phenol insertion reaction. This Michael-type reaction (27) involves another molecule of starting p-FP or m-FP and occurs without loss of halogen atom. The polymerization process becomes detectable after a 2-h reaction. It involves directly the intermediates **II** and **IV** that progressively disappear from the reaction mixture.

Comparing the reaction pattern of m-FP and p-FP after 6 h of reaction time elicits interesting differences in terms of defluorination (%F) and transformation ratio (%Tr). Despite m-FP remaining partially unreacted in these conditions, the ratio (%Tr)/(%F) amounts to 2 in both cases. This confirms that
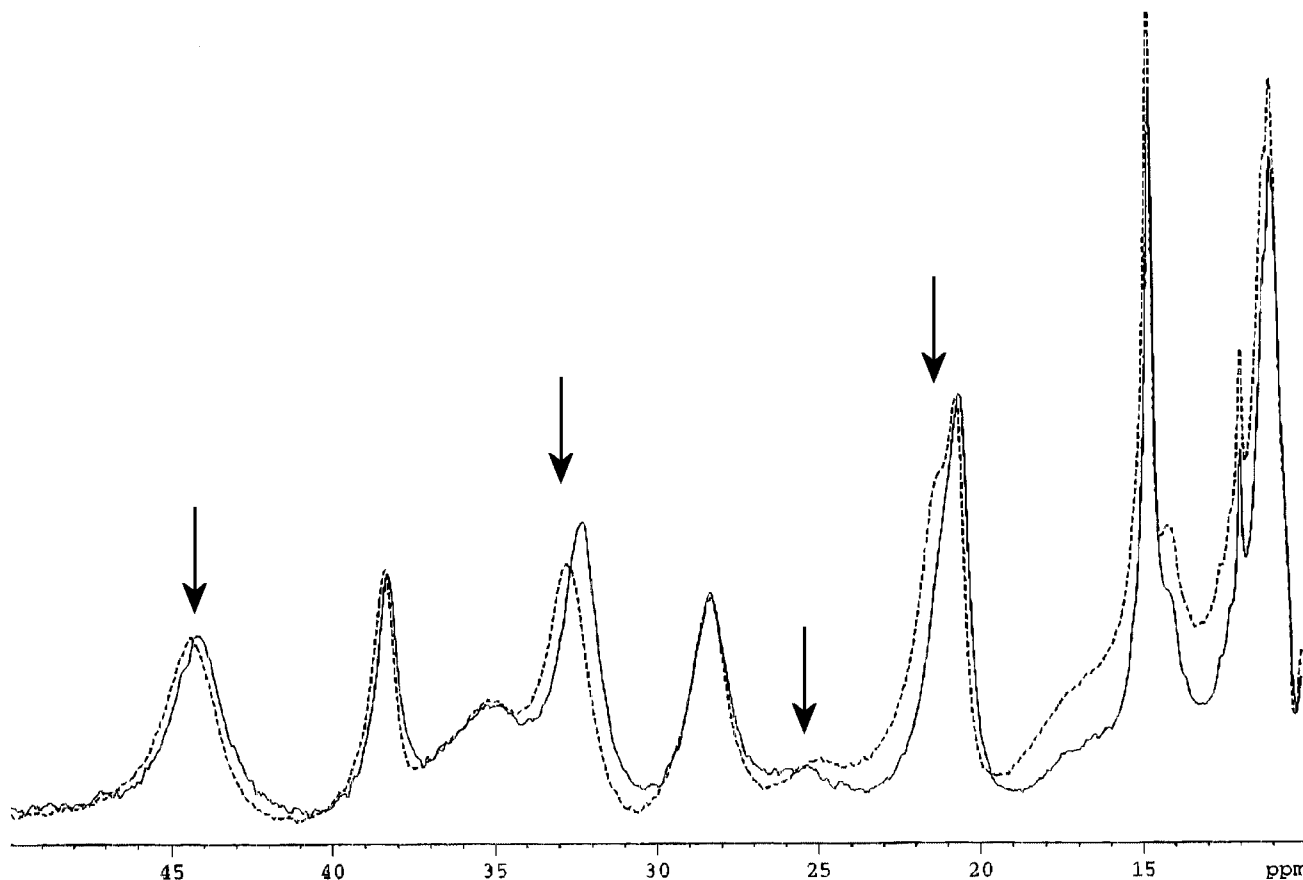
FIG. 6. **Paramagnetic ^{1}H NMR spectra of Met tyrosinase derivatives recorded at 600 MHz and 4 °C using the super-WEFT pulse sequence (32,000 scans).** The samples were buffered with 100 mM phosphate at pH 6.80. *Solid line*, native Ty$_{met}$. *Dotted line*, Ty$_{met}$ in the presence of 20 mM *o*-FP. The signals which experience upfield shifts are indicated with *arrows*.

the polymerization mechanism proceeds through the same intermediates and appears to be similar to that reported previously (20, 21) for the enzymatic oxidation of chlorophenols by mushroom tyrosinase. In order to maintain the same ratio of (%Tr)/(%F), the polymerization of **II** and **IV** must continue through a mechanism involving successive incorporation of molecules of the starting fluorophenols.

The different rate of enzymatic transformation of *m*-FP and *p*-FP is confirmed by the kinetic measurements. The kinetic profiles of formation of compound **I/III** in the absence of L-dopa show a characteristic lag, which has been systematically encountered in the Ty-catalyzed oxidation of several other phenolic substrates. The initial lag has been accounted for by considering that enzyme activation is needed when it is used in the Met form (9, 28, 29). This activation is accomplished using L-dopa because it reduces Ty$_{met}$ to Ty$_{deoxy}$, which on binding dioxygen can react with substrate (Scheme 2).

When a portion of the enzyme is already in the oxy form and/or when reducing impurities, for instance traces of catechols, are present in the substrate the phenol transformation can proceed even in absence of L-dopa. The latter effect accounts for the sigmoid curve shown in Fig. 3, because the impurities increase on increasing the substrate concentration. The activity enhancement by humic constituents such as catechol, which was reported previously (20, 21), can also be associated with these effects. The inhibitory effect of the phenols (Scheme 2), which blocks the enzyme in the Met form, increases the amount of L-dopa necessary for complete depletion of the lag phase. A 25-fold excess of L-dopa with respect to the enzyme, but still about 1/1000 the minimum substrate concen-

tration used, makes the initial activation fast enough to eliminate the lag phase throughout the concentration range of *m*-FP and *p*-FP employed, until saturation is reached. The kinetic parameters obtained, according to a Michaelis-Menten treatment, show that k_{cat} is three times larger for *p*-FP than for *m*-FP. The comparison of the k_{cat} values for *m*-FP and *p*-FP offers some additional insight into the widely accepted mechanism in which the rate-determining step involves an electrophilic attack of the phenol moiety by the Ty$_{oxy}$ form (14, 30).

The identity of the catechols formed in the oxidation of the two phenols implies that insertion of the oxygen atom into the phenol nucleus occurs in the *meta* position (to fluorine) for *p*-FP and in the *para* position (to fluorine) for *m*-FP. Thus, the fluorine dipolar effect should be much more effective for the oxygenation in *meta* position, *i.e.* it should decrease the rate of the reaction of *p*-FP more than for *o*-FP. The observed k_{cat} values show, in fact, an opposite trend. This indicates that in the rate-determining step some steric effect rules the reactivity. This effect favors the *para*-substituted phenol, carrying the same substitution pattern as the natural substrates. The *ortho*-substituted phenol is unreactive, but it binds to the active site, because it competitively inhibits the enzyme reaction (Fig. 4). To understand whether the binding mode of *o*-FP to the enzyme is similar to that of the reactive substrates, the K_m values obtained for *m*-FP and *p*-FP and the K_I value for *o*-FP have been plotted against a modified σ scale that should rationalize the fluorine substituent effect in the phenolic derivatives in terms of their relative acidity (Fig. 5) (31, 32). The observed trend suggests that the binding mode of the fluorophenols to the Ty active site is similar, and their reactivity depends on the

electronic effect modulated by the substituent position. Binding of the phenols to the enzyme is likely stabilized by interactions with protein residues. Collectively, these interactions result in weaker binding as the electron density on the phenol is reduced.

Binding of o-FP results in a relatively modest change in the paramagnetic ^{1}H NMR spectrum of Ty$_{met}$ (Fig. 6) compared, for instance, with the effects produced by halide ions and kojic acid (7, 8, 13). In particular, only a limited number of signals of Ty$_{met}$ are slightly shifted, and no sharpening of the resonances occurs. Furthermore, no new peaks likely to belong to the bonded inhibitor protons appear outside the protein envelope, even if only a complete assignment of the NMR spectrum, which is still in progress, will only provide a definitive answer. Apparently, this electron-poor phenol does not significantly modify the electronic structure of the copper site and the steric hindrance of the ortho substituent could even prevent an effective binding. Therefore, the specific interaction matrix provided by the protein envelope around the copper site could assist and enforce the binding mode, providing a rationale for the different inhibitor behavior of kojic acid and *o*-FP.

REFERENCES

1. Solomon, E. I., Sundaram, U. M., and Manchonkin, T. E. (1996) *Chem. Rev.* **96,** 2563–2605
2. Volbeda, A., and Hol, W. G. J. (1989) *J. Mol. Biol.* **209,** 249–279
3. Hazes, B., Magnus, K. A., Bonaventura, C., Bonaventura, J., Dauter, Z., Kalk, K. H., and Hol, W. G. J. (1993) *Protein Sci.* **2,** 597–619
4. Cuff, M. E., Miller, K. I., van Holde, K. E., and Hendrickson, W. A. (1998) *J. Mol. Biol.* **278,** 855–870
5. Gerdemann, C., Eicken, C., and Krebs, B. (2002) *Acc. Chem. Res.* **35,** 183–191
6. Decker, H., and Tuczek, F. (2000) *Trends Biochem. Sci.* **25,** 392–397
7. Bubacco, L., Salgado, J., Tepper, A. W., Vijgenboom, E., and Canters, G. W. (1999) *FEBS Lett.* **442,** 215–220
8. Tepper, A. W., Bubacco, L., and Canters, G. W. (2002) *J. Biol. Chem.* **277,** 30436–30444
9. Sanchez-Ferrer, A., Rodriguez-Lopez, J. N., Garcia-Canovas, F., and Garcia-Carmona, F. (1995) *Biochim. Biophys. Acta* **1247,** 1–11
10. Rodriguez-Lopez, J. N., Fenoll, L. G., Penalver, M. J., Garcia-Ruiz, P. A., Varon, R., Martinez-Ortiz, F., Garcia-Canovas, F., and Tudela, J. (2001) *Biochim. Biophys. Acta* **1548,** 238–256
11. Olivares, C., Garcia-Borron, J. C., and Solano, F. (2002) *Biochemistry* **41,** 679–686
12. van Gelder, C. W., Flurkey, W. H., and Wichers, H. J. (1997) *Phytochemistry* **45,** 1309–1323
13. Bubacco, L., Vijgenboom, E., Gobin, C., Tepper, A. W., Salgado, J., and Canters, G. W. (2000) *J. Mol. Catal. B* **8,** 27–35
14. Wilcox, D. E., Porras, A. G., Hwang, Y. T., Konrad, L., Winkler, M. E., and Solomon, E. I. (1985) *J. Am. Chem. Soc.* **107,** 4015–4027
15. Duckworth, H. W., and Coleman, J. E. (1970) *J. Biol. Chem.* **245,** 1613–1625
16. Menon, S., Fleck, R. W., Yong, G., and Strothkamp, K. G. (1990) *Arch. Biochem. Biophys.* **280,** 27–32
17. Cabanes, J., Chazarra, S., and Garcia-Carmona, F. (1994) *J. Pharm. Pharmacol.* **46,** 982–985
18. Chen, J. S., Wei, C., and Marshall, M. R. (1991) *J. Agric. Food Chem.* **39,** 1897–1901
19. Chen, J. S., Rolle, R. S., Otwell, W. S., O., B. M., and Marshall, M. R. (1991) *J. Agric. Food Chem.* **39,** 1396–1401
20. Park, J. W., Dec, J., Kim, J. E., and Bollag, J. M. (2000) *Arch. Environ. Contam. Toxicol.* **38,** 405–410
21. Park, J. W., Dec, J., Kim, J. E., and Bollag, J. M. (1999) *Environ. Sci. Technol.* **33,** 2028–2034
22. Key, B. D., Howell, R. D., and Criddle, C. S. (1997) *Environ. Sci. Technol.* **31,** 2445–2454
23. Jackman, M. P., Hajnal, A., and Lerch, K. (1991) *Biochem. J.* **274,** 707–713
24. Bertini, I., and Luchinat, C. (1996) *Coord. Chem. Rev.* **150,** 243–264
25. Boersma, M. G., Solyanikova, I. P., Van Berkel, W. J., Vervoort, J., Golovlev, E. L., and Rietjens, I. M. (2001) *J. Ind. Microbiol. Biotechnol.* **26,** 22–34
26. Clementi, V., and Luchinat, C. (1998) *Acc. Chem. Res.* **31,** 351–361
27. Peter, M. G. (1989) *Angew. Chem. Int. Ed. Engl.* **28,** 555–570
28. Espin, J. C., Garcia-Ruiz, P. A., Tudela, J., and Garcia-Canovas, F. (1998) *Biochem. J.* **331,** 547–551
29. Cooksey, C. J., Garratt, P. J., Land, E. J., Pavel, S., Ramsden, C. A., Riley, P. A., and Smit, N. P. (1997) *J. Biol. Chem.* **272,** 26226–26235
30. Decker, H., Dillinger, R., and Tuczek, F. (2000) *Angew. Chem. Int. Ed. Engl.* **39,** 1591–1595
31. Kabalpurwala, K., and Milburn, R. (1966) *J. Am. Chem. Soc.* **88,** 3224–3227
32. Leffler, J. E., and Grunwald, E. (1963) *Rates and Equilibria of Organic Reactions*, Wiley Interscience, New York